A Wide-Angle and Circularly Polarized Beam-Scanning Antenna Based on Microstrip Spoof Surface Plasmon Polariton Transmission Line

Dong-Fang Guan, Peng You, Qingfeng Zhang, Zhong-Hao Lu, Shao-Wei Yong, and Ke Xiao

***Abstract*—In this letter, a wide-angle beam-scanning antenna with circular polarization (CP) characteristic is proposed. The antenna consists of two layers. Microstrip spoof surface plasmon polariton (SPP) is introduced on the bottom layer as a slow-wave feeding line. A series of circular patches are placed on the top layer as radiating elements. Simulated and measured results indicate that beam-scanning angle of the proposed antenna is improved and CP beam-scanning ability is obtained by introducing perturbation on the radiating elements. In the operating band of 11–15 GHz, measured scanning angle of the fabricated antenna is from –32° to +34°. The antenna axial ratio (AR) is below 3 dB at the corresponding beam direction, and gain is above 12.8 dBi over the whole band. It has potential applications in radar and wireless communication systems for simple structure, low-cost fabrication, wide beam-steering, and CP properties.**

***Index Terms*—Beam-scanning antenna, circular polarization (CP), surface plasmon polariton (SPP), wide angle.**

I. Introduction

FREQUENCY beam-scanning antennas are widely used in modern wireless communication systems, such as radar and point-to-point and satellite communication systems, due to their ability to generate different beam points with variation of frequencies [1]. Leaky-wave antennas (LWAs) are one type of simple beam-scanning antenna and have received much attention for their low profile, compact structure, low cost, and easiness of integration with planar circuits [2]–[4].

Conventional LWAs have limited beam-scanning range only along the forward direction. It is challenging to enhance the beam-scanning range of LWAs. Composite right-/left-handed structures were applied in the LWA design to realize beam scanning from the backward to the forward direction [5]. However, most of the metamaterial-based beam-scanning antennas suffer from complicated structure or have difficulty in maintaining balance between frequencies. Employing slow-wave lines is another way to enhance beam-scanning angle of LWAs [6]–[8]. A low-loss slow-wave printed meander line based on the even-mode bilateral broadside-coupled suspended microstrip line was used in [6], and the antenna achieved a beam-scanning angle from –27.5° to +46°. In [7] and [8], meandering lines were introduced in substrate-integrated waveguide LWAs to realize wide-angle beam steering. Due to high field confinement and slow-wave feature, spoof surface plasmon polariton (SPP) can be used to improve the beam scanning angle of LWA. SPP is a special kind of slow-wave structure in optical frequencies with advantage of confining light in subwavelength. Using periodical subwavelength structure to mimic the characteristics of SPP, spoof SPP has been realized in microwave band [9], [10]. Periodic SPP cells were used as radiating part in LWA of [11] to generate a radiating space harmonic with forward, backward, and broadside radiation against frequency change. In [12], a groundless SPP slow-wave line was proposed to feed a circular-patch array. Wide-angle beam scanning from backward direction to forward direction was achieved. However, the radiation patterns are bidirectional both in [11] and [12] because there are no grounds.

On the other hand, the aforementioned beam-scanning antennas are all linear polarization (LP). Circular polarization (CP) beam is difficult to be scanned compared with the LP one. The challenge is to maintain a pure CP mode within a wide scan region [13]. Some CP LWAs were realized mainly based on two separated LP elements with coupler or delay line [13], [14]. In this letter, a wide-angle and circularly polarized beam-scanning antenna based on microstrip SPP slow-wave structure is proposed. The antenna consists of two layers. Using SPP slow-wave line with ground as the feeding line on the bottom layer, the antenna radiation patterns are unidirectional and can be steered with enhanced angle. The radiating elements composed of circular patches are placed on the top layer, and CP beam scanning is realized by introducing perturbation on the radiating elements. Experimental results show that the proposed CP antenna has an operating band of 11–15 GHz with a beam-scanning angle from –32° to +34° and axial ratio (AR) below 3 dB at each maximal radiating direction. Moreover, the measured gain is in the range of 12.8–14.2 dBi.

II. Antenna Design

The geometry of the proposed CP beam-scanning antenna is shown in Fig. 1. It is designed on the F4BM-2 printed

Manuscript received May 31, 2017; revised July 3, 2017; accepted July 21, 2017. Date of publication July 25, 2017; date of current version August 28, 2017. This work was supported in part by the Natural Science Foundation of Hunan Province, China, under Grant 2017JJ3364, in part by the National Natural Science Foundation of China under Grant 61601487, in part by Guangdong NSF for DYS (2015A030306032), and in part by Guangdong STD funds (2016TQ03X839). *(Corresponding authors: Peng You; Qingfang Zhang.)*

D.-F. Guan, P. You, Z.-H. Lu, S.-W. Yong, and K. Xiao are with the College of Electronic Science and Engineering, National University of Defense Technology, Changsha 410073, China (e-mail: gdfguandongfang@163.com; ypnudt@126.com; luzhnudt@163.com; ysw_nudt@vip.126.com; xiaoke_e@hotmail.com).

Q. Zhang is with the Department of Electronics and Electrical Engineering, Southern University of Science and Technology, Shenzhen 518055, China (e-mail: zhang.qf@sustc.edu.cn).

Color versions of one or more of the figures in this letter are available online at http://ieeexplore.ieee.org.

Digital Object Identifier 10.1109/LAWP.2017.2731877

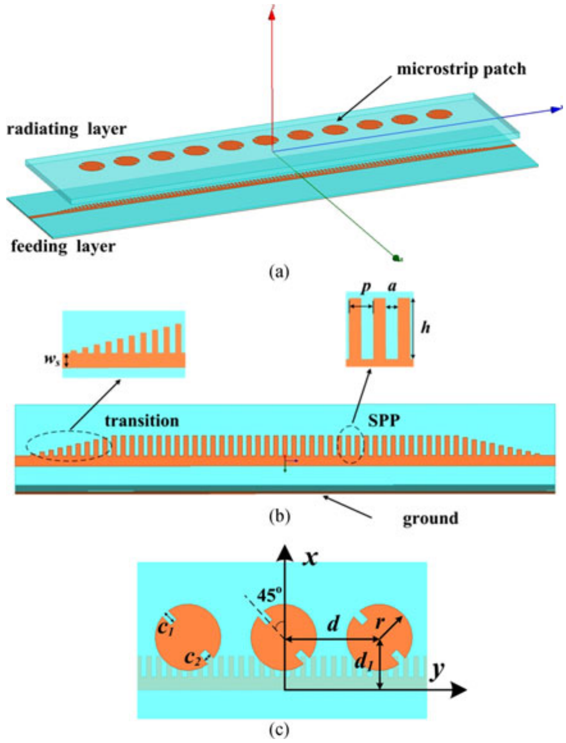

Fig. 1. Geometry of the proposed CP beam scanning antenna: (a) perspective view; (b) feeding layer; (c) radiating layer.

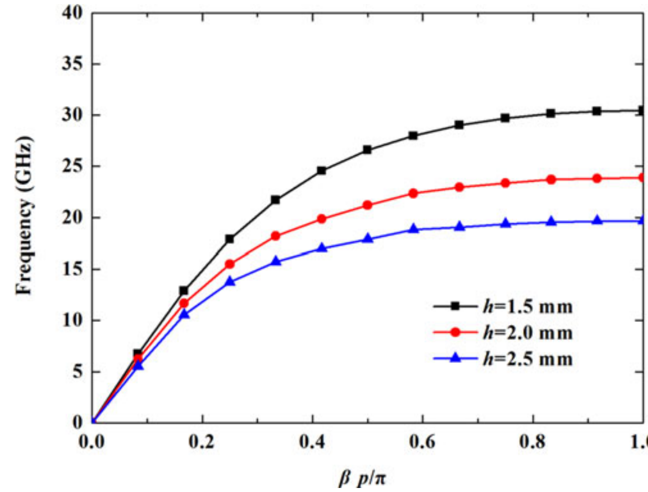

Fig. 2. Dispersion diagram of the proposed SPP unit.

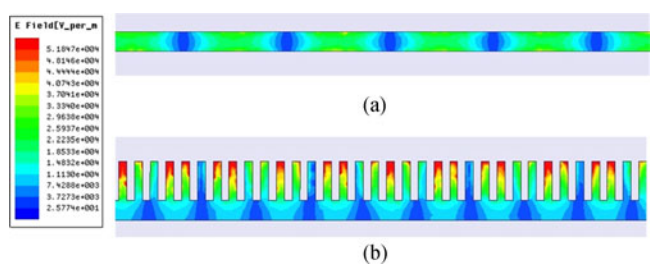

Fig. 3. Simulated electric-field distributions: (a) microstrip line; (b) SPP slow-wave line.

circuit board with relative dielectric constant $\varepsilon_r = 2.65$ and loss tangent $\tan\delta = 0.001$. As exhibited in Fig. 1(b), an SPP slow-wave line is designed on the bottom substrate with thickness $h_1 = 0.5$ mm, which is formed by introducing a series of corrugated metallic strips on one side of microstrip line. The period of SSP structure is *p*. The groove width and the depth of SPP unit are *a* and *h*, respectively. There are transition sections between SSP and microstrip line to realize effective modes transformation, in which the groove depth varies from 0 to *h* in gradient. For convenience of measurement, the microstrip line with width w_s is 50 Ω.

It has been proved that such periodic metallic grooves can support and propagate surface plasmon mode in microwave frequency. The dispersion characteristic of the proposed SPP unit is analyzed with Ansoft HFSS, and the simulated result is depicted in Fig. 2. The SPP parameters are set at $a = 0.5$ mm and $p = 1$ mm in simulation. It can be observed that the dispersion curves deviate gradually to slow-wave region with β increasing, where β is the propagation constant of the SPP mode. The curves finally reach up to different upper cutoff frequencies as the groove depth *h* changes. Moreover, the slow-wave effect of SPP can also be affected by the parameters *a* and *p*. The simulated electric-field distributions of the proposed SPP and microstrip lines are compared in Fig. 3. Owing to the slow-wave feature, the wavelength of microstrip SPP line is only half of the microstrip line's wavelength.

The radiating part is designed on the top substrate with thickness $h_2 = 1.5$ mm. A row of circular metallic patches is the radiating elements. The number of elements is 11 in our design. As shown in Fig. 1(c), the patch radius is *r* and the space between adjacent elements is *d*. The antenna resonant frequency is mainly determined by the patch size. In terms of the empirical equation, the radius *r* is initially set as

$$r = \frac{k_{11} c}{2\pi\sqrt{\varepsilon_r} f} \tag{1}$$

where k_{11} is the eigenvalue of TM_{11} mode, *c* is the velocity of the light in vacuum, and *f* is the center frequency. By tuning the element space *d* to realize radiating in phase at the center frequency, symmetrical beam scanning about the boresight can be achieved.

The circular patches are fed by SPP line through coupled feeding. When the circular patches are placed at the side of SPP on the same layer like the design in [12], it is difficult to realize the effective coupling between the patches and SPP. As shown in Fig. 4, the reflection coefficient S_{11} is lower than –10 dB, while the transmission coefficient S_{21} is above –10 dB in the whole operating band for the single-layer design. It means part energy is received by the terminal port and the antenna efficiency is low. In our design, the radiating elements are placed above the SPP feeding line and coupling effect can be optimized by adjusting the position parameter d_1. It can be seen from Fig. 4 that the transmission coefficient S_{21} can be restrained below –10 dB in a large band when d_1 is 2 mm. In this case, most energy is radiated out. The other reason for the two-layer design is to realize circularly polarized radiation. As shown in Fig. 1(c), the circular patches are truncated at the diagonal corners with depth of c_1 and width of c_2. Except for the parameters c_1 and c_2, optimizing the position parameter d_1 can improve the purity of CP further.

The SPP slow-wave line is used here to enhance the beam-scanning range. To verify the angle enhancement, the simulated

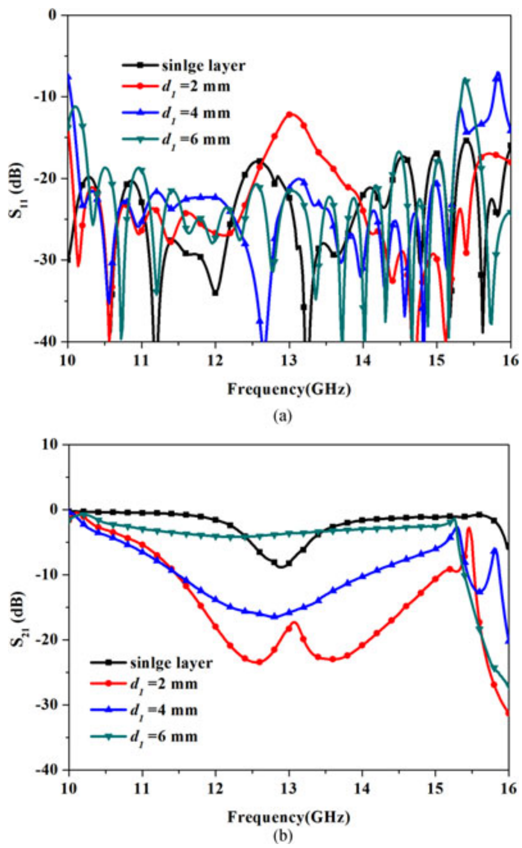

Fig. 4. Simulated reflection coefficients (S_{11}) and transmission coefficients (S_{21}) of a single-layer antenna and the proposed double-layer antenna with different d_1.

TABLE I
DIMENSION VALUES OF THE CP ANTENNA (UNIT: mm)

p	a	h	h_1	h_2	w_s
1	0.5	2	0.5	1.5	1.26
r	d	d_1	c_1	c_2	
3.2	9.3	3.5	1.5	0.8	

radiation patterns of the proposed antenna and the antenna with the same radiating elements fed by microstrip line are compared in Fig. 5. The antenna fed by microstrip line covers an operating band of 11–15 GHz with a beam-scanning angle of 27° from –18° to +9° as shown in Fig. 5(a). The gain is in the range of 13.4–15.7 dBi. Within the same operating band, the beam-scanning angle of the proposed antenna is enhanced to 68° from –31° to +37° and the gain is from 13.9 dBi to 15.6 dBi, as shown in Fig. 5(b). The simulated results indicate that the antenna scanning angle is improved more than two times based on the SPP slow-wave structure.

III. Simulated and Measured Results

To validate correctness of the analysis above, the proposed CP beam-scanning antenna is fabricated and tested. After optimization with Ansoft HFSS, geometry parameters of the antenna are listed in Table I. A sample is fabricated, and the antenna photograph is shown in Fig. 6. Two layers of the antenna are aligned and fixed by screws for measurement. The simulated and

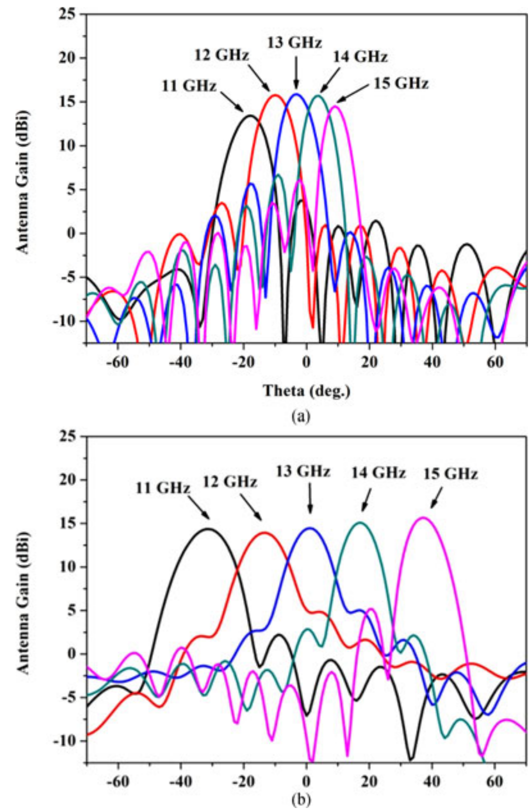

Fig. 5. Comparison of radiation patterns between antennas fed by (a) microstrip line and (b) SPP slow-wave line.

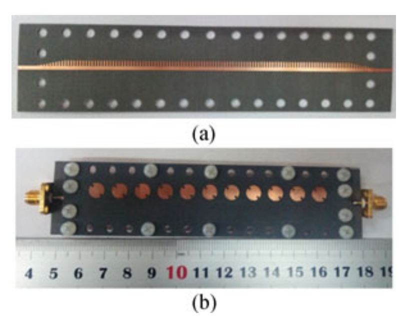

Fig. 6. Photograph of the fabricated CP antenna: (a) bottom layer; (b) top layer.

measured reflection and transmission coefficients are shown in Fig. 7. It can be seen from the figure that the trend of the measured curves is accordant with the simulated ones. The measured S_{11} and S_{21} are both below –10 dB covering the required operating band of 11–15 GHz. It means that most energy is radiated out by the antenna elements.

The antenna radiation patterns and ARs are measured in a chamber with far-field setup from 11 to 15 GHz. The measured radiation patterns are plotted in Fig. 8, and the simulated and measured antenna ARs versus theta are shown in Fig. 9. A more detailed comparison between simulated and measured radiation performance is listed in Table II. It can be seen that the simulated beam angle is scanned from –31° to +37° and the measured scanning angle is in the range from –32° to +34°. It is proved that wide angle scanning ability is realized for the proposed CP antenna. The antenna simulated gain reaches up to 13.9–15.6 dBi,

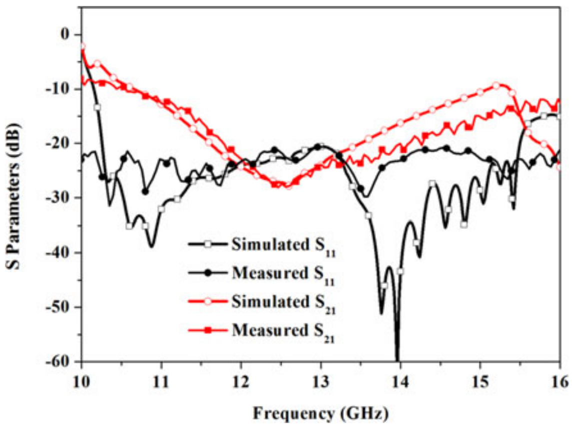

Fig. 7. Simulated and measured *S*-parameters of the proposed CP antenna.

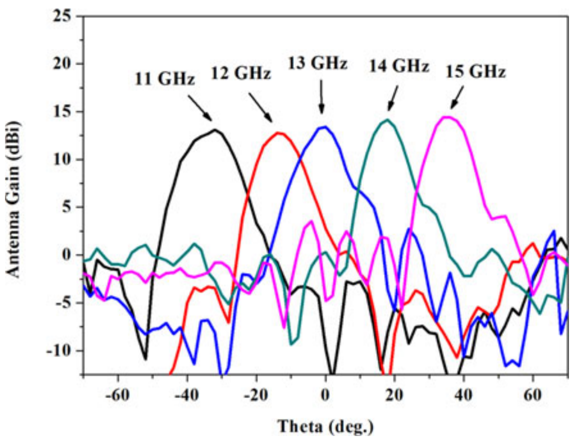

Fig. 8. Measured radiation patterns of the proposed CP antenna.

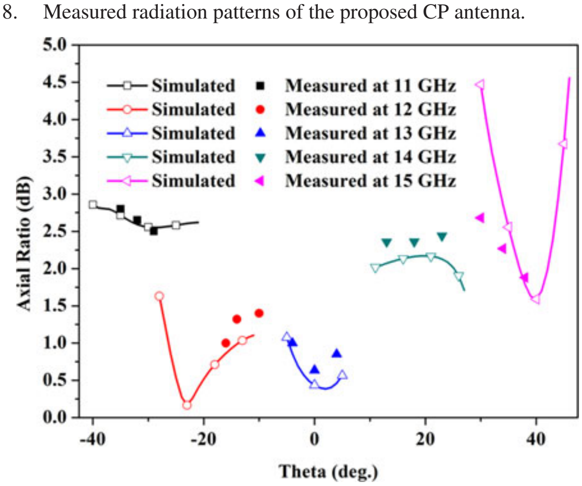

Fig. 9. Simulated and measured ARs of the proposed CP antenna.

TABLE II
SIMULATED AND MEASURED RESULTS OF THE CP ANTENNA

Frequency (GHz)	Beam Direction (degree)		AR (dB)		Gain (dBi)	
	Sim.	Mea.	Sim.	Mea.	Sim.	Mea.
11	−31	−32	2.5	2.6	14.4	13.1
12	−13	−14	1.0	1.3	13.9	12.8
13	0	0	0.4	0.6	14.4	13.6
14	+17	+18	2.1	2.4	15.1	14.2
15	+37	+34	2.2	2.3	15.6	13.9

while the measured gain is in the range of 12.8–14.2 dBi. The discrepancy between the simulated and measured results is mainly due to the insertion losses caused by the antenna fabrication and the connectors, which are not considered in simulation. The variation of the measured gain at different frequencies is less than 2 dB. The simulated and measured ARs are lower than 3 dB in the direction of the expected beams. As was expected, the CP characteristic is verified for the fabricated antenna.

IV. CONCLUSION

In this letter, a wide-angle and circularly polarized beam-scanning antenna is proposed. A microstrip SPP slow-wave line with ground is used as the feeding structure to enhance antenna beam-scanning range and realize unidirectional radiation. The radiating elements constituted by a series of circular patches are designed on the other layer to achieve CP radiation. The experimental results indicate that the proposed antenna has wide angle scanning ability and CP radiation feature. In the operating band of 11–15 GHz, antenna measured scanning angle is from –32° to +34° with AR below 3 dB and gain above 12.8 dBi. This antenna has potential applications in radar and wireless communication systems for its advantages of simplicity in design, low cost in fabrication, and wide beam-steering and CP properties.

REFERENCES

[1] D. R. Jackson, A. A. Oliner, and C. Balanis, *Modern Antenna Handbook*. Hoboken, NJ, USA: Wiley, 2008.
[2] J. L. Gomez-Tornero, F. D. Quesada-Pereira, and A. Alvarez-Melcon, “Analysis and design of periodic leaky-wave antennas for the millimeter waveband in hybrid waveguide-planar technology,” *IEEE Trans. Antennas Propag.*, vol. 53, no. 9, pp. 2834–2842, Sep. 2005.
[3] D. R. Jackson, C. Caloz, and T. Itoh, “Leaky-wave antennas,” *Proc. IEEE*, vol. 100, no. 7, pp. 2194–2206, Jul. 2012.
[4] F. Monticone and A. Alu, “Leaky-wave theory, techniques, and applications: From microwaves to visible frequencies,” *Proc. IEEE*, vol. 103, no. 5, pp. 793–821, May 2015.
[5] W. Q. Cao, Z. N. Chen, W. Hong, B. N. Zhang, and A. J. Liu, “A beam scanning leaky-wave slot antenna with enhanced scanning angle range and flat gain characteristic using composite phase-shifting transmission line,” *IEEE Trans. Antennas Propag.*, vol. 62, no. 11, pp. 5871–5875, Nov. 2014.
[6] L. Cui, W. Wu, and D. G. Fang, “Printed frequency beam-scanning antenna with flat gain and low sidelobe levels,” *IEEE Antennas Wireless Propag. Lett.*, vol. 12, pp. 292–295, 2013.
[7] L. Chiu, W. Hong, and Z. Kuai, “Substrate integrated waveguide slot array antenna with enhanced scanning range for automotive application,” in *Proc. Microw. Conf. Asia Pacific*, 2009, pp. 1–4.
[8] W. Q. Cao, W. Hong, Z. N. Chen, B. N. Zhang, and A. J. Liu, “Gain enhancement of beam scanning substrate integrated waveguide slot array antennas using a phase-correcting grating cover,” *IEEE Trans. Antennas Propag.*, vol. 62, no. 9, pp. 4584–4591, Sep. 2014.
[9] J. Pendry, L. Martin-Moreno, and F. Garcia-Vidal, “Mimicking surface plasmons with structured surfaces,” *Science*, vol. 305, pp. 847–848, 2004.
[10] F. Garcia-Vidal, L. Martin-Moreno, and J. Pendry, “Surfaces with holes in them: New plasmonic metamaterials,” *J. Opt., Pure Appl. Opt.*, vol. 7, pp. S97–S101, 2005.
[11] A. Kianinejad, Z. N. Chen, and C. W. Qiu, “A single-layered spoof plasmon leaky wave antenna with consistent gain,” *IEEE Trans. Antennas Propag.*, vol. 65, no. 2, pp. 681–687, Feb. 2017.
[12] J. Y. Yin *et al.*, “Frequency-controlled broad-angle beam scanning of patch array fed by spoof surface plasmon polaritons,” *IEEE Trans. Antennas Propag.*, vol. 64, no. 12, pp. 5181–5189, Dec. 2016.
[13] Y. Cheng, W. Hong, and K. Wu, “Millimeter-wave half mode substrate integrated waveguide frequency scanning antenna with quadri-polarization,” *IEEE Trans. Antennas Propag.*, vol. 58, no. 6, pp. 1848–1855, Jun. 2010.
[14] H. Lee, J. H. Choi, C. M. Wu, and T. Itoh, “Compact single radiator CRLH-inspired circularly polarized leaky-wave antenna based on substrate-integrated waveguide,” *IEEE Trans. Antennas Propag.*, vol. 63, no. 10, pp. 4566–4572, Oct. 2015.